Correlation between excitation temperature and electron temperature with two groups of electron energy distributions

Hoyong Park,[1] S. J. You,[2] and Wonho Choe[1,a)]
[1]*Department of Physics, Korea Advanced Institute of Science and Technology, 335 Gwahangno, Yuseong-gu, Daejeon 305-701, Republic of Korea*
[2]*Korea Research Institute of Standards and Science, P. O. Box 102, Yuseong-gu, Daejeon 305-600, Republic of Korea*

(Received 18 February 2010; accepted 11 August 2010; published online 12 October 2010)

The relationship between the electron excitation temperature (T_{exc}) determined by optical emission spectroscopy and the electron temperature (T_e) using a rf-compensated Langmuir probe was investigated in argon capacitively coupled plasmas. In the experiment performed at the gas pressure range of 30 mTorr to 1 Torr and the rf power range of 5–37 W, the electron energy probability function (EEPF) obtained from the probe current versus voltage characteristic curve showed two energy groups of electrons. The measured EEPF demonstrated that the electron energy distribution changed from Druyvesteyn to single Maxwellian as the discharge current was increased and from bi-Maxwellian to Druyvesteyn as the pressure was increased. As a result, T_{exc} showed a tendency identical to that of T_e of the high energy part of electrons as pressure and rf power were varied. This suggests that electron temperature can be determined from the measured T_{exc} through a calibration experiment by which the ratio between electron and excitation temperatures is measured.
 [doi:10.1063/1.3486093]

I. INTRODUCTION

One of the most prevalent and versatile means of measuring important plasma parameters in low temperature plasmas is electrical probes. Use of these probes is, however, occasionally limited owing to difficulties in analyses under some circumstances, perturbation of the plasmas, etc. Recently, industrial demands for large area and/or volume plasmas are rapidly increasing, for instance, processing plasmas for liquid crystal flat panel displays of which size reaches more than 2 m. Since application of the plasma diagnostics conventionally employed in smaller scale plasmas may be restricted to these larger size plasmas, alternative diagnostic methods are needed and especially optical emission spectroscopy (OES) becomes of greater importance because it may offer means of overcoming the aforementioned limitations.

There are a number of previous studies that investigated the relationship between electron temperature (T_e) obtained by Langmuir probes and excitation temperature (T_{exc}) obtained by OES in various low pressure plasmas including glow discharge plasma,[1] inductively coupled plasma,[2] and capacitively coupled plasma (CCP).[3] According to these earlier studies, T_{exc} is in good agreement with T_e in argon plasmas, which may suggest that T_{exc} diagnostic can be a good alternative for T_e diagnostic.[4,5] However, the prior studies only dealt with the single Maxwellian distribution of electron energy. Since there are many occasions in which electron energy distributions exhibit departure from Maxwellian, investigation on the relationship between T_{exc} and T_e in the plasmas with non-Maxwellian electron energy distributions will make an important addition to the related studies.

In this study, the correlation between the argon atom excitation temperature (measured by OES) and the electron temperature (measured by a Langmuir probe) in two different energy regions deduced from the Druyvesteyn and bi-Maxwellian electron energy probability functions is investigated in argon plasmas.

Section II describes the experimental setup, and the results and discussions for both the excitation temperature and the electron temperature are presented in Sec. III. The conclusion is given in Sec. IV.

II. EXPERIMENTAL

The plasma was generated in a vacuum chamber with two parallel electrodes that had diameters of 140 mm (Fig. 1). The gap distance between the electrodes was approximately 40 mm. The upper electrode was powered through an impedance matching network from 5 to 37 W at a fixed frequency of 13.56 MHz using a radio frequency (rf) generator (ENI, A1000–1971), while the lower electrode was grounded. The argon operating pressure was ranged from 30 mTorr to 1 Torr. The detailed explanation of the plasma source is found in our previous report.[6] In order to obtain the visible spectrum emitted from the plasma, a CHROMEX 250is spectrometer with a 250 mm focal length and 1200 groove/mm grating, and a charge coupled device detector (SBIG, ST-9XE) was used. The spectral resolution of the spectrometer was 0.375 nm with an entrance slit width of 50 μm. Prior to the detection, the optical collection system was calibrated with 546.07 nm of Hg I line of a mercury lamp. A plano-convex lens of a focal length of 500 mm was mounted on an optical rail to focus the plasma image onto the entrance slit of the spectrometer. The sampling area in

a)Author to whom correspondence should be addressed. Electronic mail: wchoe@kaist.ac.kr.

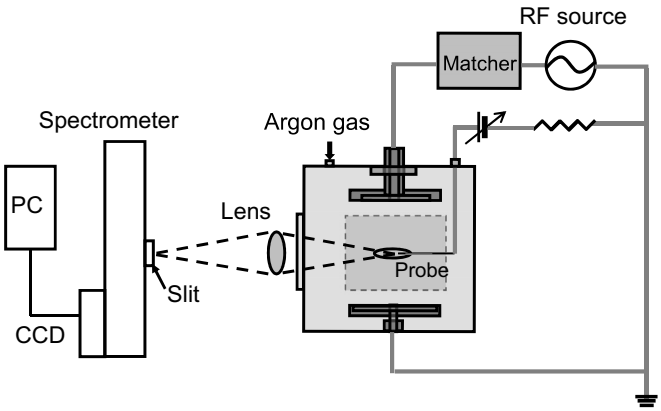

FIG. 1. Schematic of the experimental setup consisting of an OES system (spectrometer and a plano-convex lens) and a Langmuir probe. A lens of 500 mm focal length was used to focus the same diagnostic area of the probe measurement. The sampling area traced back to the plasma is a rectangle of 0.05×20 mm^2 of which location corresponds to that of the Langmuir probe.

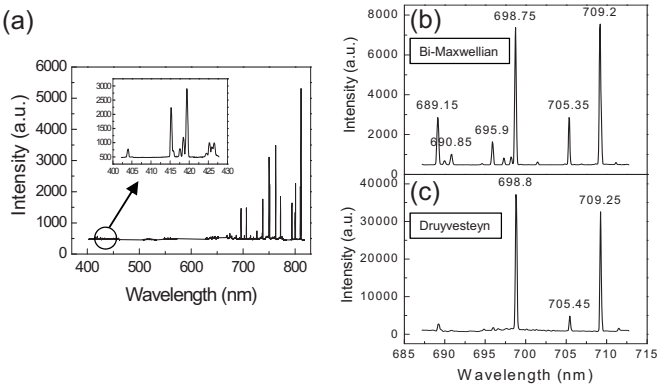

FIG. 2. (a) A typical emission spectrum of Ar I lines. The inserted plot shows the wavelength range from 400 to 430 nm. (b) Partial spectra of Ar I lines at the pressures of (b) 10 mTorr and (c) 1 Torr at a fixed power of 22 W.

the plasma for OES was 0.05 mm $\times$ 20 mm of which location corresponded to that of the Langmuir probe.

A single, cylindrical, rf-compensated Langmuir probe was placed at the center of the two electrodes to obtain the current (I) versus voltage (V) characteristic curves of the plasma. The probe measurement system was equipped with a small probe tip consisting of a tungsten wire of 5 mm in length and 0.1 mm in diameter and a floating-loop reference probe to reduce the rf distortion in the probe characteristics. For rf compensation, two self-resonant chokes with peak impedances at 13.56 and 27.12 MHz were used. Since probe contamination also distorts the probe characteristics, which typically causes severe distortion at the peak in the measured second derivative of the probe characteristics, the probe was cleaned periodically by drawing a large current to heat the probe tip.

III. EXPERIMENTAL RESULTS AND DISCUSSIONS

The excitation temperature T_{exc} is evaluated from the measured relative emission intensity I_{jk} of the transition from level j to level k. Assuming a Boltzmann distribution of the population of the atomic levels, I_{jk} is given by[7–9]

$$I_{jk} = \frac{hc}{\lambda}\frac{n g_j A_{jk}}{U(T_{\mathrm{exc}})}\exp\left(-\frac{E_j}{T_{\mathrm{exc}}}\right) \tag{1}$$

which is rearranged as

$$\ln\left(\frac{I_{jk}\lambda}{A_{jk}g_j}\right) = 1.4388 \times \frac{E_j[\mathrm{cm}^{-1}]}{T_{\mathrm{exc}}[K]} + \mathrm{const.} \tag{2}$$

A Boltzmann plot is based on Eq. (2) to represent natural logarithm of I_{jk} against the energy E_j, in which each data point corresponds to each emission line of a specific wavelength λ. The excitation temperature T_{exc} is evaluated from the inverse of the slope of the Boltzmann plot. Here, h is the Planck constant, n is the number density of bound electrons in all ionization states, $U(T_{\mathrm{exc}})$ is the partition function, c is the speed of light in vacuum, λ is the wavelength of the corresponding transition, A_{jk} is the Einstein probability spontaneous emission coefficient between the excited levels of j and k. Also E_j and g_j are the energy difference and the statistical weight of a level j, respectively.

There are reports regarding the experimental uncertainties in T_{exc} determination when an insufficient number of emission data points is used in the Boltzmann plot.[10,11] To achieve greater measurement accuracy, the range of the energy difference between the high and low energy groups should be as large as possible.[8] In this study, 34 measured Ar I emission lines were used for Boltzmann plot in the wavelength range from 415 to 811 nm, where 415 nm ($5p \rightarrow 4s$ transition) is close to the Ar I ionization limit. A typical Ar emission spectrum is shown in Fig. 2(a) obtained at 13 W rf power and 500 mTorr gas pressure.

For T_e measurement using a single Langmuir probe, the electron energy probability function (EEPF) $g_p(\varepsilon)$ was acquired by differentiating the I-V curve twice. By taking the natural logarithm of the obtained EEPF

$$\ln g_p(\varepsilon) = \mathrm{const.} - \frac{\varepsilon}{T_e}, \tag{3}$$

where ε is the electron energy and T_e is found from the inverse of the slope. In this experiment, a typical I-V curve was obtained by averaging more than 256 measurements for good statistics. Depending on discharge conditions, the I-V characteristic curves demonstrated not only single Maxwellian but also Druyvesteyn and bi-Maxwellian electron distributions having two electron energy groups: a group of low energy electrons $(T_e)_{\mathrm{low}}$ at equilibrium in the bulk plasma and a group of high energy electrons $(T_e)_{\mathrm{high}}$ emitted from the cathode and accelerated over the sheath into the bulk plasma. This two electron energy distributions are the typical characteristic of CCPs with large rf electric fields and secondary electron emissions caused by electrode ion bombardment and other factors.[12]

Figures 2(b) and 2(c) depict the spectral range near 700 nm, showing intensity difference between bi-Maxwellian (at 10 mTorr) and Druyvesteyn (at 1 Torr) distributions. The Druyvesteyn distribution is characterized by a shift toward higher electron energies, as compared to the Maxwellian.[13] Since the electrons in the high energy group have significant

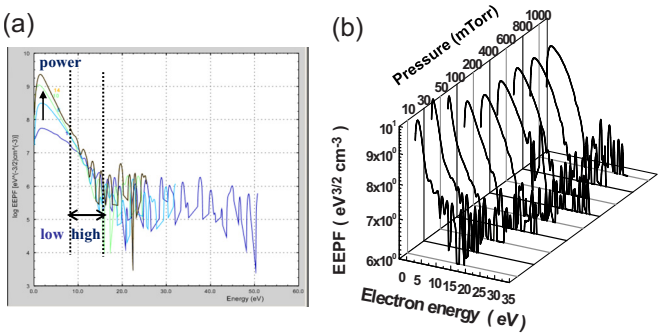

FIG. 3. (Color online) (a) The measured EEPFs with power at a fixed pressure of 500 mTorr. (b) EEPF evolution with pressure at fixed power of 22 W.

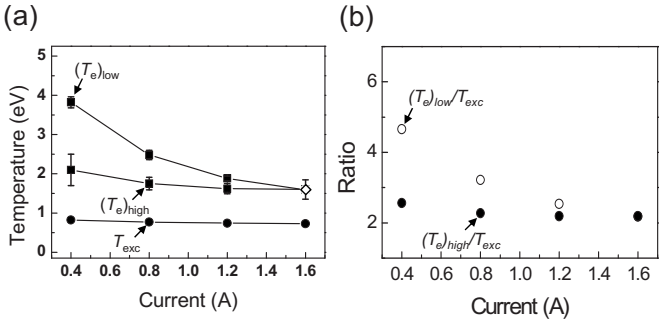

FIG. 4. (a) Excitation temperature (T_{exc}), high energy electron temperature $(T_e)_{high}$, and low energy electron temperature $(T_e)_{low}$ against discharge current and (b) their ratios. The Ar pressure was 500 mTorr.

impact on the overall reaction rates, especially in excitation, the intensities measured in Druyvesteyn distribution [Fig. 2(c)] are much higher than those in bi-Maxwellian distribution [Fig. 2(b)]. As we will see later in Fig. 5, this intensity difference may contribute to the fact that $(T_e)_{high}$ in bi-Maxwellian distribution observed at lower pressures is higher than that in Druyvesteyn distribution observed at higher pressures.

Figure 3(a) demonstrates the measured EEPF, showing a change from the Druyvesteyn to the single Maxwellian distribution as the input power was increased. The energy ranges of the high and low energy electron groups are in 1–8 and 8–12 eV, respectively. Figure 3(b) indicates the evolution of the EEPF as the argon pressure was changed at a fixed rf power. As seen in the figure, EEPFs vary considerably in shape, rapidly changing from the bi-Maxwellian to the Druyvesteyn distribution at a threshold pressure of about 100 mTorr. This can be explained in terms of electron heating mode transition with the pressure.[14] At low pressure, the high energy electrons, which are able to overcome the dc ambipolar potential barrier, can penetrate into the sheath region where the collisionless electron heating strongly takes place and thereby be effectively heated. On the contrary, the low energy electrons remaining in the bulk gain energy just through collisional heating process that is usually weak because of a low collision frequency at low pressure and a small electric field in the bulk. Therefore, the electron distribution at the low pressure discharge is normally characterized by the bi-Maxwellian electron distribution having two distinct electron groups. On the other hand, in a high-pressure regime where collisional heating is dominant, the electron sees the rf electric fields as dc fields rather than oscillating fields during its mean free time if the collision time is much shorter than the rf period. In this condition, electron energy gain ($\Delta\varepsilon$) from the field is proportional to the electron mean free path (λ), $\Delta\varepsilon = eE\lambda$ where e is the electron charge and E is the rf electric field. The mean free path of low energy electrons is longer than that of high energy electrons because of the Ramsauer minimum of collision cross section near 0.3 eV in the Ar discharge. Therefore, compared with the high energy electrons, the low energy electrons are effectively heated. As a result, the EEDF exhibits a Druyvesteyn-type form. As pressure increases, therefore, the electron distribution changes from the bi-Maxwellian distribution to Druyvesteyn-like distribution. The transition pressures for the electron heating mode[14] for our experiment are about 0.4 and 0.1 Torr, respectively. We can see that these two results are well consistent with each other when we apply the scaling law, $pd = p(L-2s) = \text{const}$, where p is the gas pressure, d is the plasma bulk length, L is the discharge gap, and s is the sheath length (for simplicity we set $2s = 1$ cm). Because the plasma length (d) expands from 1 to 3 cm, the transition pressure has to shrink, $0.4/3 = 0.133 - 0.1$.

Both T_{exc} and T_e are presented as a function of discharge current at 500 mTorr in Fig. 4(a) and their ratios are shown in Fig. 4(b). At this pressure, the measured EEPF demonstrated that the electron energy distribution of the plasma changed from the Druyvesteyn (represented by squares) to the single Maxwellian [represented by empty diamond at 1.6 A where merge of $(T_e)_{low}$ and $(T_e)_{high}$ occurs] as the discharge current was increased. As presented in the figure, $(T_e)_{low}$ shows a steep rate of decay while $(T_e)_{high}$ exhibits only a slight change. This abrupt change in the EEPF is well known in rf discharges as the discharge experiences transition into the γ-mode from the α-mode.[12] In the γ-mode, ion bombardment leads to secondary electron emission from the rf electrodes, and electron acceleration and multiplication within the rf sheath produce intensive ionization in the bulk plasma, accompanied by a drop in electron temperature, especially drastic decrease of $(T_e)_{low}$. It should be noted from Fig. 4(b) that the ratio between $(T_e)_{high}$ and T_{exc} remains almost constant, indicating that the trend of T_{exc} is similar to that of $(T_e)_{high}$ as the discharge current varies.

Shown in Fig. 5 are both T_{exc} and T_e as a function of gas pressure at a fixed power of 22 W. At this operating condition, the trend of $(T_e)_{high}$ is almost opposite to that of $(T_e)_{low}$ due to the aforementioned difference in the electron heating process. At low pressure, the high energy electrons are actively heated by collisionless stochastic heating while the low energy electrons are confined in the reduced rf field caused by oscillating boundaries between bulk and sheath regions. At high pressure, on the other hand, the low energy electrons are heated by collisional heating. As a result, $(T_e)_{high}$ is decreased while $(T_e)_{low}$ is increased as the pressure is raised as shown in Fig. 5(a). This phenomenon is reflected in the EEPF, i.e., the measured EEPF varies considerably in

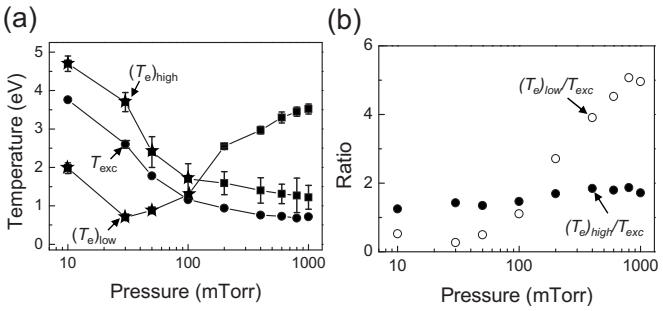

FIG. 5. (a) The excitation and two electron temperatures and (b) their ratios against the pressure. The rf power was 22 W.

terms of its shape from the bi-Maxwellian at low pressure (represented by stars) to the Druyvesteyn at high pressure (represented by squares).

It is also seen that T_{exc} shows the same tendency as $(T_e)_{high}$ as the pressure is varied. The ratio between T_{exc} and $(T_e)_{high}$, depicted in Fig. 5(b), remains almost constant at approximately 1.8, which is very much different from $(T_e)_{low}/T_{exc}$. As mentioned previously, each data point in the Boltzmann plot corresponds to each Ar I emission line of a specific wavelength with the electron excitation energy as abscissa. The electron excitation energy range in Fig. 2(b) is 105 463–124 609 cm^{-1}, which is converted as 13.09–15.46 eV. This electron excitation energy range corresponds to the high electron energy range in the EEPFs with two energy groups of electrons. For instance, the high energy electron group appears in 8–15 eV in the Druyvesteyn distribution presented in Fig. 3(a). It means that excitation of Ar atoms and thus emission of 415–811 nm photons is due to these high energy group electrons. This is why the trends of $(T_e)_{high}$ and T_{exc} are similar. As opposed to the low pressure, the electron energy loss to Ar atom excitation is comparable with or larger than the electron heating in the high pressure, thus the depletion of the tail of EEDF becomes observable, as shown the figure below (EEPF at 400 mTorr at the discharge center).[15] The EEPF shows the depletion of high energy tail of EEPF clearly above the 11.5 eV which is the first excitation energy threshold of an Ar atom.

In our results, although T_{exc} showed the similar trend as $(T_e)_{high}$, T_{exc} was always lower than $(T_e)_{high}$. It may be explained by the fact that although the high energy group electrons play a significant role in exciting argon atoms, they are unable to effectively deliver their energy to the argon atoms due to inelastic collisions with the atoms in low electron density CCPs. In addition, since the electron density in our experiment ($\sim 10^9$ cm^{-3}) was lower than the critical density given by Griem criterion, departure from local thermodynamic equilibrium can reduce T_{exc}.[16]

IV. CONCLUSIONS

Comparisons of T_{exc} and T_e were performed utilizing OES and a Langmuir probe. At low rf power (<37 W) CCP, EEPFs with two electron energy groups with two different temperatures $(T_e)_{high}$ and $(T_e)_{high}$ were observed with a bi-Maxwellian distribution at low pressure (below 100 mTorr) and a Druyvesteyn distribution at high pressure (above 200 mTorr). The evolution from Druyvesteyn to single-Maxwellian was also observed as the discharge experiences transition from α-mode to γ-mode at 500 mTorr, indicating that secondary emission electrons from the rf electrodes produce intensive ionization in the bulk plasma, thus leading to a drop in $(T_e)_{low}$.

The large sheath potential, stochastic electron heating, and secondary electrons create a high energy tail in the EEPF in the low power CCPs, as presented by Langmuir probe diagnostics. The trend of this high energy part in the EEPF is shown to be similar to that of the excitation temperature when varying the gas pressure and discharge current. In addition to the similarity of the trends in the two temperatures, $(T_e)_{high}$ can be determined through a calibration experiment by which the $(T_e)_{high}/T_{exc}$ ratio is measured.

ACKNOWLEDGMENTS

This work was supported partially by National R&D Program through the National Research Foundation of Korea (NRF) funded by the Ministry of Education, Science and Technology (Grant No. 2010-0020037) and partially by the Samsung LCD Business, Korea. The authors would like to thank Dr. C. R. Seon for his experimental assistance and valuable discussions.

[1] A. Bogaerts, A. Quentmeier, N. Jakubowski, and R. Gijbels, Spectrochim. Acta, Part B **50**, 1337 (1995).
[2] V. M. Donnelly, J. Phys. D: Appl. Phys. **37**, R217 (2004).
[3] M. A. Naveed, N. U. Rehman, S. Zeb, S. Hussain, and M. Zakaullah, Eur. Phys. J. D **47**, 395 (2008).
[4] M. Numano, O. Furukawa, and I. Michiyoshi, Plasma Phys. **13**, 992 (1971).
[5] W. K. McGregor and L. E. Brewer, Phys. Fluids **9**, 826 (1966).
[6] S. J. You, C. W. Chung, K. H. Bai, and H. Y. Chang, Appl. Phys. Lett. **81**, 2529 (2002).
[7] S. Y. Moon, W. Choe, H. S. Uhm, Y. S. Hwang, and J. J. Choi, Phys. Plasmas **9**, 4045 (2002).
[8] W. Lochte-Holtgreven, *Plasma Diagnostics* (AIP, New York, 1995).
[9] P. W. J. M. Boumans, *Inductively Coupled Plasma Emission Spectroscopy Part 2* (Wiley, New York, 1987), Chap. 10.
[10] N. K. Joshi, S. N. Sahasrabudhe, K. P. Sreekumar, and N. Venkatramani, Meas. Sci. Technol. **8**, 1146 (1997).
[11] P. Jamroz and W. Zyrnicki, Surf. Coat. Technol. **201**, 1444 (2006).
[12] V. A. Godyak, R. B. Piejak, and B. M. Alexandrovich, Plasma Sources Sci. Technol. **1**, 36 (1992).
[13] N. Spyrou and C. Manassis, J. Phys. D **22**, 120 (1989).
[14] V. A. Godyak and R. B. Piejak, Phys. Rev. Lett. **65**, 996 (1990).
[15] U. Kortshagen, C. Busch, and L. D. Tsendin, Plasma Sources Sci. Technol. **5**, 1 (1996).
[16] A. Yanguas-Gil, J. Cotrino, and A. R. Gonzalez-Elipe, J. Appl. Phys. **99**, 033104 (2006).